SERI/TP-252-2847
UC Category: 59b
DE86004430

# Blockage of Natural Convection Boundary Layer Flow in a Multizone Enclosure

**Douglas Scott**
**Ren Anderson**
**Richard S. Figliola**

**February 1986**

Prepared for AIAA/ASME
Heat Transfer and
Thermophysics Conference
Boston, Massachusetts
June 2-4, 1986

**Prepared under Task No. 3751.210**
**FTP No. 527**

**Solar Energy Research Institute**
A Division of Midwest Research Institute

1617 Cole Boulevard
Golden, Colorado 80401-3393

Prepared for the
**U.S. Department of Energy**
Contract No. DE-AC02-83CH10093

Printed in the United States of America
Available from:
National Technical Information Service
U.S. Department of Commerce
5285 Port Royal Road
Springfield, VA 22161

Price: Microfiche A01
Printed Copy A02

Codes are used for pricing all publications. The code is determined by the number of pages in the publication. Information pertaining to the pricing codes can be found in the current issue of the following publications, which are generally available in most libraries: *Energy Research Abstracts, (ERA); Government Reports Announcements* and Index (*GRA* and I); *Scientific and Technical Abstract Reports (STAR);* and publication, NTIS-PR-360 available from NTIS at the above address.

# BLOCKAGE OF NATURAL CONVECTION BOUNDARY LAYER FLOW IN A MULTIZONE ENCLOSURE

Douglas Scott
Graduate Research Assistant
Department of Mechanical Engineering
Clemson University
Clemson, South Carolina

Ren Anderson
Staff Engineer
Thermal Research Branch
Solar Energy Research Institute
Golden, Colorado
Assc. Member ASME

Richard S. Figliola
Associate Professor
Department of Mechanical Engineering
Clemson University
Clemson, South Carolina
Member ASME

## ABSTRACT

Two separate mechanisms can be responsible for natural convection flow between the hot and cold zones of a multizone enclosure: (1) bulk density differences created by temperature differences between the fluid in the hot and cold zones (bulk density driven regime) and, (2) thermosyphon "pumping" generated by boundary layers or plumes (boundary layer driven regime).

This paper reports the results of an experimental study that examines the transition between flow regimes, as a function of aperture size, in a two-zone enclosure with heated and cooled end walls. A constant heat flux boundary condition was maintained on one vertical end wall, and an isothermal cold temperature sink was maintained on the opposite vertical end wall. All of the remaining surfaces were highly insulated.

The transition between the boundary layer driven regime and the bulk density driven regime was established as a function of the geometry of the aperture in the partition that separated the hot and cold zones. The results demonstrate that transition from the boundary layer driven regime to the bulk density driven regime is caused by blockage of the boundary layer flow, when the area of the flow aperture is reduced below a critical value.

A simple flow model has been developed which predicts that the critical aperture area for the onset of flow blockage is directly proportional to the number of active heat transfer surfaces and inversely proportional to the Rayleigh number which characterizes the level of heating and cooling provided to the active heat transfer surfaces.

## NOMENCLATURE

| | |
|---|---|
| A | area |
| $A_H$ | aperture height ratio, h/H |
| $A_s$ | aspect ratio, H/L |
| $A_W$ | aperture width ratio, w/W |
| C | discharge coefficient for aperture |
| $c_p$ | specific heat at constant pressure |
| g | acceleration due to gravity |
| h | height of aperture (y-dimension) |
| H | height of test cell/partition (y-dimension) |
| k | thermal conductivity |
| L | length of test cell (x-dimension) |
| N | number of active heat transfer surfaces |
| Nu | Nusselt number, $\frac{q''H}{k\Delta T}$ |
| $\overline{Nu}$ | Nusselt number, $\frac{q''H}{k\Delta \overline{T}}$ |
| Pr | Prandlt number, $\frac{\mu c_p}{k}$ |
| q" | average heat flux per unit area |
| q | total heat flux, q"A |
| Ra* | flux modified Rayleigh number, $\frac{g\beta H^4 q''}{\nu\alpha k}$ |
| $\Delta T$ | midheight temperature difference between the heated and cooled end walls |
| $\overline{\Delta T}$ | temperature difference between the fluid in the middle of the hot and cold zones at the midheight of the aperture |
| w | width of aperture (z-dimension) |
| W | width of test cell (z-dimension) |
| x,y,z | non-dimensional, spatial coordinates, X/L, Y/H, Z/W |

Greek

$\alpha$ thermal diffusivity, $\frac{k}{\rho c_p}$

$\beta$ coefficient of thermal expansion

$\rho$ density

$\nu$ kinematic viscosity, $\frac{\mu}{\rho}$

$\mu$ viscosity

$\delta$ boundary layer thickness

$\theta$ $\frac{T - T_C}{T' - T_C}$

Superscript

' midpoint

Subscripts

bl boundary layer

**INTRODUCTION**

There has been a strong interest in the behavior of natural convection in enclosures because of the important role that natural convection plays in determining the performance of thermal insulation systems, solar collectors, thermal storage systems, building space conditioning systems, and the study of smoke and fire spread in buildings. Recent reviews on the topic of natural convection in enclosure geometries have been prepared by Catton[1], Ostrach[2], and Churchill[3]. Reviews of research directly related to smoke and fire spread in buildings have been given by Quintiere[4] and by Yang and Lloyd[5].

In many of the applications cited above, the convective heat transfer process is complicated by the presence of internal partitions. There are two primary mechanisms that can drive natural convection flows through apertures in multizone enclosures: (1) bulk density differences between hot and cold zones, and (2) motion pressure differences generated by natural convection boundary layers or plumes. The terminology "motion pressure" refers to pressure differences generated by fluid motion above and beyond hydrostatic pressure differences.

Researchers who have examined smoke and fire spread in buildings have long recognized the existence of two types of flow behavior, depending upon whether the flow aperture is large or small[6]. Satoh, Lloyd and Yang[7] have conducted numerical calculations that span the range from the "small opening limit" to the "large opening limit" for the case of a cubic enclosure with a gas burner located centrally on the floor of the enclosure.

Brown and Solvason[8] conducted heat transfer measurements of bulk density driven flow in an air-filled enclosure that was divided into hot and cold regions by a single partition with a centrally located rectangular opening. Using inviscid calculations and assuming isothermal fluid reservoirs on either side of the partition, they demonstrated that the heat transfer through the partition could be correlated by the relationship.

$$\overline{Nu} = \left(\frac{C}{3}\right)^{2/3} A_W^{2/3} A_H \left(R_a^* P_r\right)^{1/3} \qquad (1)$$

The constant C appearing in Eq. (1) is the discharge coefficient for the aperture and was reported by Brown and Solvason to have values in the range $0.6 \le C \le 0.98$.

The Nusselt number $\overline{Nu}$ in Eq. (1) is based upon the temperature difference between the fluid reservoirs on either side of the partition, at the mid-height of the aperture. Bulk density flow models similar to Eq. (1) have been used as the basis of analysis of air flow in solar buildings[9,10].

Multizone flows driven by natural convection boundary layers have been studied by several investigators. Two-dimensional apertures have been considered by Janikowski, Ward, and Probert[11]; Bejan and Rossie[12]; Nansteel and Greif[13]; Bajorek and Lloyd[14]; Chang, Lloyd, and Yang[15]; and Lin and Bejan[16]. All of these studies were experimental, with the exception of that of Chang, Lloyd, and Yang, which was a finite difference model of a geometry similar to the experimental work of Bajorek and Lloyd.

Chang, Lloyd and Yang[15] considered partitions that extended equal distances from the floor and ceiling of a square cavity, and calculated the reduction in heat transfer that occurred as the height of the partitions was increased. Lin and Bejan provided a perturbation solution valid in the limit $Ra \to 0$ in addition to their experimental results.

Nansteel and Greif[13] and Lin and Bejan[16] conducted experiments at large Rayleigh numbers and demonstrated that the presence of a partition between zones tends to damp out the natural convection boundary layer flow in sub regions that are subjected to stable thermal boundary conditions. This effect reduces the wall area that is exposed to the primary boundary layer flow and results in an overall reduction in the convective heat transfer between the hot and cold surfaces on either side of the partition. Nansteel and Greif[17] correlated their data to include this effect. Their correlation, expressed in terms of the present notation, is

$$Nu = 0.929\, A_H^{0.332}\, Ra^{*\,0.172} \qquad (2)$$

$$1/4 \le A_H \le 1 \qquad (3)$$

$$A_W = 0.093\ ,\ 0.25 \le A_H \le 1.0 \qquad (4)$$

The Nusselt number Nu in Eq. (2) is based upon the temperature difference between the hot and cold end walls.

The only previous three-dimensional study is that of Nansteel and Greif[17] who considered a partition with a variable width opening. Nansteel and Greif[17] compared their three dimensional results to their previous study with $A_W = 1.0$ (Nansteel and Greif[13]) and found that the heat transfer between zones did not depend strongly upon the width of the aperture, for $A_W \ge 0.093$.

A comparison between Eq. (1) and Eq. (2) demonstrates that the natural convection flow regime that governs the flow through the aperture (bulk density driven or boundary layer driven) has a strong impact upon the geometric dependence of the heat transfer coefficient. In the bulk density driven regime [Eq. (1)] the heat transfer between zones depends strongly upon both the aperture height ratio $A_H$ and the aperture width ratio $A_W$. In the boundary layer regime [Eq. (2)] the heat transfer between zones depends weakly upon the aperture height ratio and appears to be independent of the aperture width ratio. Because of these differences, it is important to be able to predict when a multizone flow is in the bulk density driven or boundary layer driven regime. The primary objective of the present study is to determine the transition between the bulk density driven regime and boundary layer driven regime, as a function of

vertical aperture geometry in a simple two-zone enclosure with heated and cooled end walls.

Boundary Layer Flow Blockage Model

Nansteel and Greif[17] have demonstrated that heat transfer between two zones in the boundary layer regime is nearly independent of the width of the aperture between zones for $A_W \geq 0.093$ and $0.25 \leq A_H \leq 1.0$. However, as the width of the aperture is reduced below values considered by Nansteel and Greif, the boundary layer flow will eventually be blocked. Flow blockage will result in the formation of large temperature differences across the aperture and cause a transition from boundary layer driven to bulk density driven convection.

The onset of boundary layer flow blockage can be estimated by comparing the total cross-sectional area required by the boundary layer flow to the area of the aperture between zones. If the area of the aperture is smaller than the area required by the boundary layer flow, then the boundary layer flow will have to accelerate to pass through the aperture. The additional driving force required to convect the flow through the aperture can be provided only by the creation of bulk density differences between the hot and cold zones of the enclosure.

The flow area required by the boundary layers on heated and cooled surfaces can be calculated by summing the product of the thickness and width of each boundary layer in the enclosure

$$A_{bl} = \sum_{n=1}^{N} (\delta W)_n \tag{5}$$

According to the model described above, flow blockage will occur when

$$\frac{A_{bl}}{hw} = \frac{\sum_{n=1}^{N} (\delta W)_n}{hw} \sim 1 \tag{6}$$

For laminar flow it can be shown that the natural convection boundary layer thickness next to a vertical surface is scaled by the relationship

$$\frac{\delta}{H} \sim \frac{1}{(Ra^*)^{1/5}} \tag{7}$$

If we assume that the height, width, and average heat flux from each active surface are H, W, and q", then the flow blockage criteria expressed by Eq. (6) can be rearranged into the simple form

$$A_W A_H \sim \frac{N}{Ra^{*1/5}} \tag{8}$$

The lefthand side of Eq. (8) is the ratio of the area of the aperture to the cross-sectional area of the enclosure and N is the number of active heat transfer surfaces in the enclosure. Equation (8) predicts that the onset of flow blockage is directly proportional to the number of active heat transfer surfaces and is inversely proportional to the Rayleigh number which characterizes the natural convection flow.

## EXPERIMENTAL APPARATUS AND PROCEDURE

The experimental measurements were performed in an approximately cubic water-filled test cell with L = 56.5 cm, H = 58.4 cm, and W = 57.2 cm (Fig. 1).

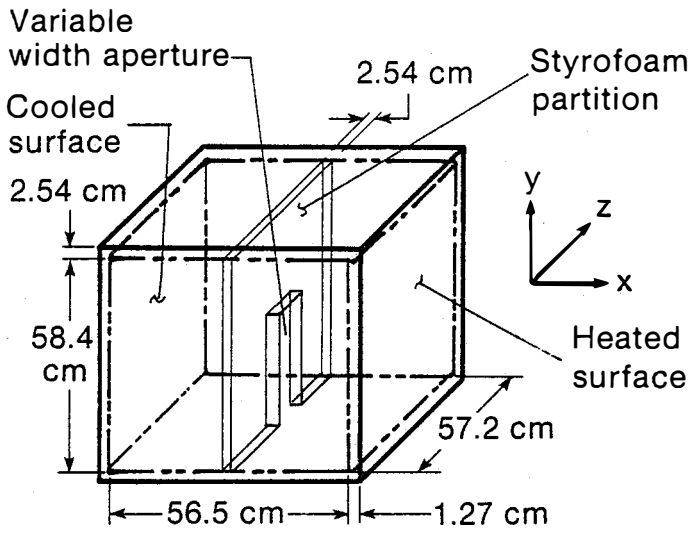


**Figure 1. Schematic of Test Cell and Partition**

Two opposing, vertical walls and the cell bottom were constructed of nickel-plated aluminum 1.27 cm thick. The remaining vertical walls were constructed of plate glass 0.64 cm thick. The top of the cell was constructed of plexiglass 2.54 cm thick. A constant heat flux boundary condition was maintained on one vertical aluminum wall and an isothermal temperature sink was maintained on the opposite vertical aluminum wall. All other boundaries were highly insulated.

All fluid properties used in the calculation of nondimensional quantities were evaluated at the average of the midpoint temperature of the hot and cold wall. A neoprene gasket of 0.32 cm thickness separated the vertical aluminum walls from the floor of the test cell. The vertical dividing partition was constructed of styrofoam 2.54-cm thick, 58.4-cm high, and 57.2-cm wide. A half height rectangular aperture was cut into the middle of the partition (Fig. 1). The width of the aperture was increased from 0.32 cm until it extended across the entire width of the test cell. Tests were also conducted without an aperture in the partition and with the partition completely removed from the test cell.

The constant heat flux boundary condition on the heated wall was maintained with 16 electric resistance zone heaters wired in parallel and attached to the outside of the heated aluminum wall. Power input to the heaters was monitored by wattmeters calibrated to within ±2%. The temperature variations on the cold wall were kept to within 2% of the average cooled wall temperature by circulating chilled water through two zones of channels milled into a 2.54-cm plexiglass plate bolted to the back of the aluminum wall.

To reduce heat loss through the cell walls, the test cell was insulated with 5.1 cm of styrofoam insulation and 15.2-cm of fiberglass batting. The heat loss from the test cell was measured to be 2.2 W per degree centigrade temperature difference between the average heat cell temperature and the ambient. All tests were conducted keeping the average temperature of the test cell as close as possible to the ambient temperature to minimize loss. The power input to the test cell was varied between 50 watts and 600 watts. The heat loss from the test cell was generally less than 5% of the end to end heat transfer and was subtracted from the power input to the test cell when the data were analyzed. The conductance of the partition

was measured in the absence of an aperture and found to be 0.5 watts per degree C temperature difference between the fluid on either side of the partition. Conduction through the partition was generally less than 1% of the total end to end heat transfer in the test cell.

Temperature was measured in the hot end wall, the cold end wall, and in the floor of the test cell by thermocouples buried 0.16 cm from the inside wall surface and located along the vertical axis at z = W/2. Additional temperature measurements were made at other z locations on the vertical end walls to ensure that temperature on the walls did not vary in the z direction. Two thermocouple rakes were used to measure temperature simultaneously at nine vertical locations at the midpoint of the hot and cold zones on either side of the partition. The amount of heat conduction in the floor of the test cell was calculated based upon the measured temperature distribution in the floor and was found to be less than 1% of the total end to end heat transfer.

The temperature and the power input to the heaters were measured with a microcomputer-based data acquisition system. An ice point reference was used to correct for any drift in the calibration of the temperature measurement channels on the data acquisition system. The experimental error associated with temperature measurements using this system is estimated to be ±0.2°C. Power input, wall temperature, and rake temperature were monitored every 2 minutes and displayed graphically on the computer monitor. Generally, it took about 10 hours for the test cell to reach steady state when the power setting or aperture geometry was changed. After steady state had been reached, five sets of data were taken over a period of about 10 minutes and averaged to give the final data point for each power setting and aperture width ratio.

The major sources of experimental error are summarized in Table 1. These errors correspond to a 6% error in determination of the Nusselt number and nondimensional temperatures that are reported in the results.

**Table 1. Experimental Errors**

| | |
|---|---|
| Temperature | ±0.2°C |
| Conduction in floor and partition | ±2% |
| Temperature difference | ±2% |
| Power input | ±2% |

## Experimental Results

Figure 2 shows the nondimensional temperature θ plotted as a function of the vertical (y) coordinate at two locations: (1) in the middle of the hot zone x = L/4, z = w/2 (Fig. 2a), and (2) in the middle of the cold zone x = 3L/4, z = w/2 (Fig. 2b). The nondimensional temperature θ is defined to be the difference between the local temperature and the cold wall temperature, divided by the difference between the temperature at half height (y = H/2) and the cold wall.

Figure 2a demonstrates the dramatic increase in temperature that occurs in the upper portion of the hot zone when a half-height partition is present. This temperature increase results from a reduction of the strength of the boundary layer flow in the stably stratified region bounded by the top of the test cell, the upper half of the partition, and the upper half of the heated wall. Dye injection studies confirmed the presence of a large slowly rotating cell in this region. The formation of the cell has been described previously by Lin and Bejan[16] and by Nansteel and Greif[17]. As the width of the aperture between the hot and cold zones is reduced, the temperature profiles in Fig. 2a indicate that the level of thermal stratification in the hot zone is gradually reduced. As the boundary layer flow is blocked, the hot zone tends to become more isothermal and approaches the temperature of the hot end wall.

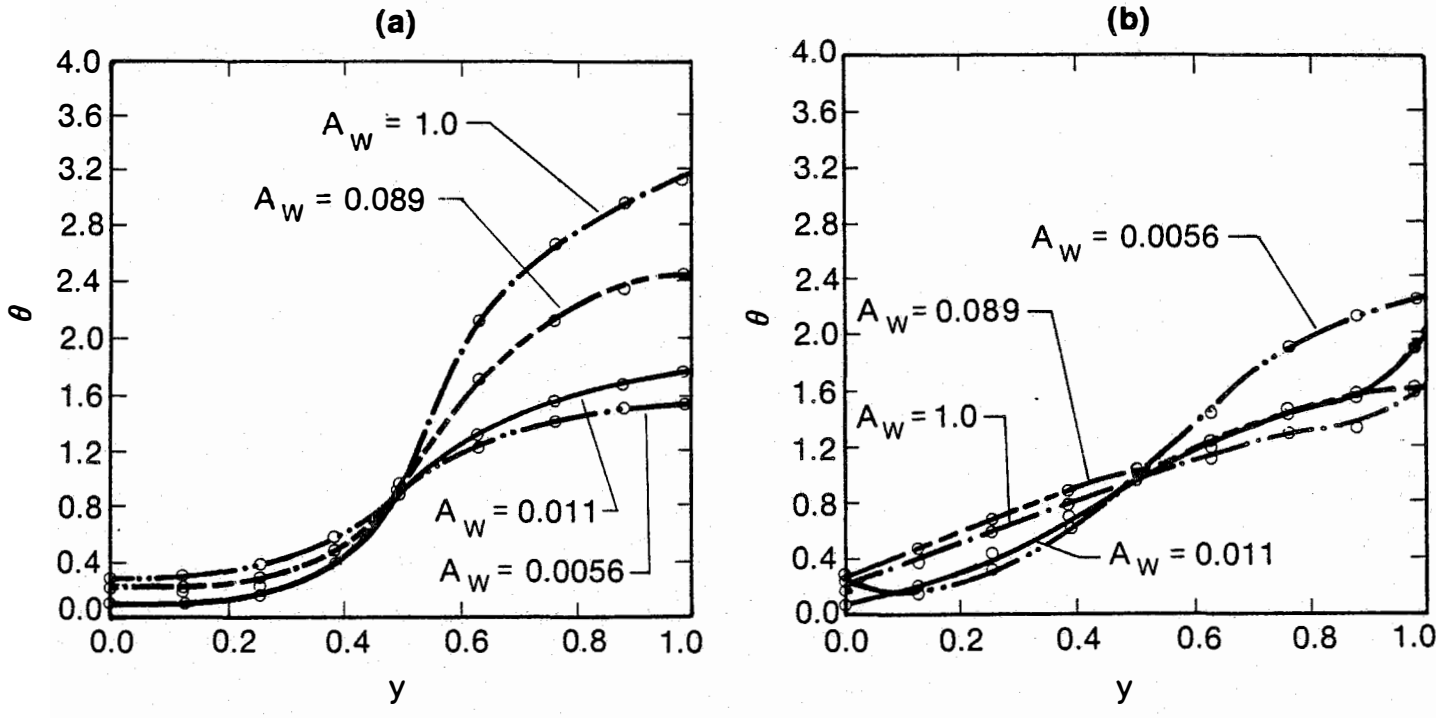


**Figure 2. Dimensionless Temperature, θ, as a Function of Vertical Location (a) Hot Zone (b) Cold Zone**

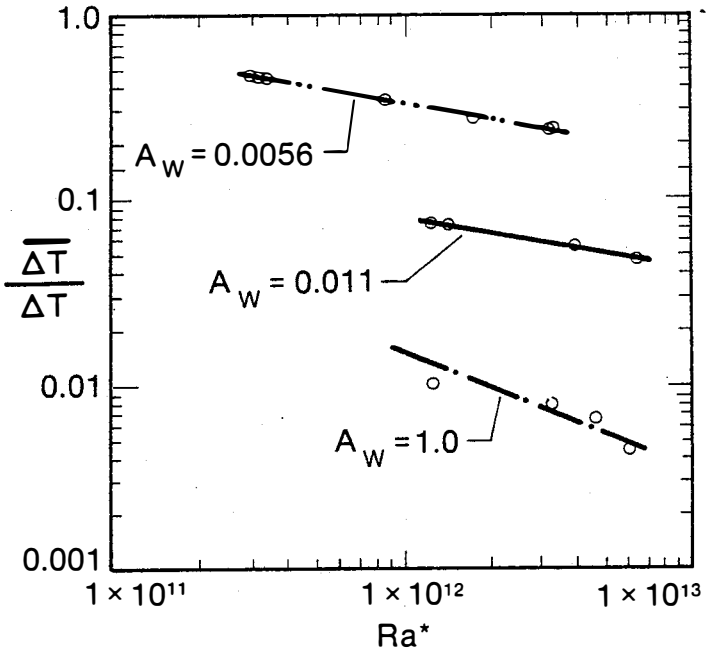


**Figure 3. Comparison of Fluid Difference, $\overline{\Delta T}$ With End Wall Temperature Difference, $\Delta T$**

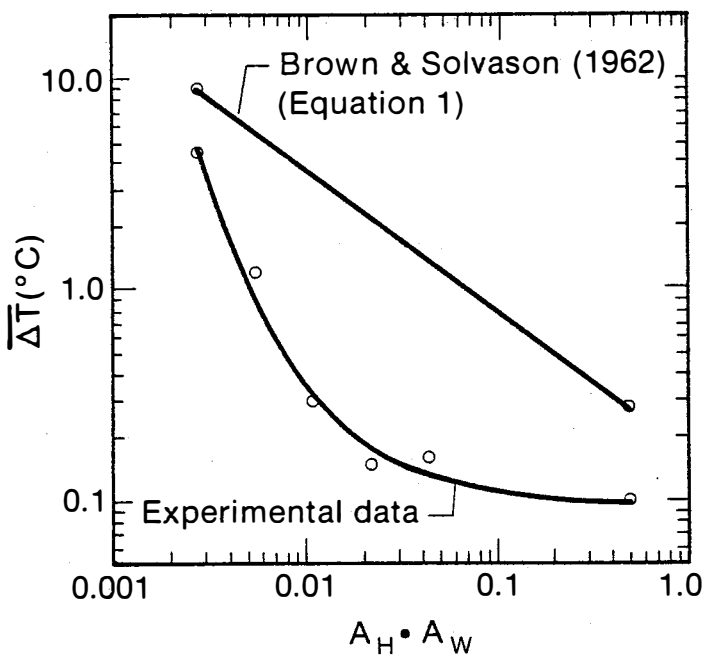


**Figure 4. Comparison Between Temperature Differences Predicted by the Bulk Density Flow Model and Experimental Results**

Figure 3 compares the temperature difference between the fluid in the hot and cold zones at the midheight of the aperture (y = H/4) with the temperature difference between the hot and cold end walls at y = H/2, as a function of Ra*. When the size of the aperture is reduced, the fluid temperature difference between the hot and cold zones rapidly approaches the temperature difference between the hot and cold end walls. The ratio $\overline{\Delta T}/\Delta T$ decreases as the Rayleigh number increases, indicating that high Rayleigh number flows are less likely to be blocked than small Rayleigh number flows, in qualitative agreement with the trend predicted by Eq. (8).

In Figure 4, the zone-to-zone temperature difference, $\overline{\Delta T}$, measured during the experiment is compared to the zone-to-zone temperature difference for a bulk density driven flow, as calculated from Eq. (1). The data and calculation shown in Fig. 4 are for a constant zone-to-zone convective energy transfer of 500 watts.

As the size of the flow aperture between zones is reduced, the bulk density flow model [Eq. (1)] predicts that the temperature difference required to transfer a given amount of heat across the aperture will have to increase steadily. However, the experimental observations indicate that the temperature difference between zones does not increase until a critical aperture area is reached. This critical aperture area is approximately 2% of the total cross-sectional area of the test cell. This result demonstrates that boundary layer "pumping" can have a significant impact upon the transport of fluid between hot and cold zones. The boundary layers can transport fluid through the aperture without requiring a large zone-to-zone temperature difference, provided that the aperture area is larger than the critical value for the onset of flow blockage.

Average Nusselt numbers are plotted as a function of Rayleigh number in Fig. 5. The heat transfer results, when the partition is completely removed from the test cell ($A_H$ = 1), are shown in addition to data

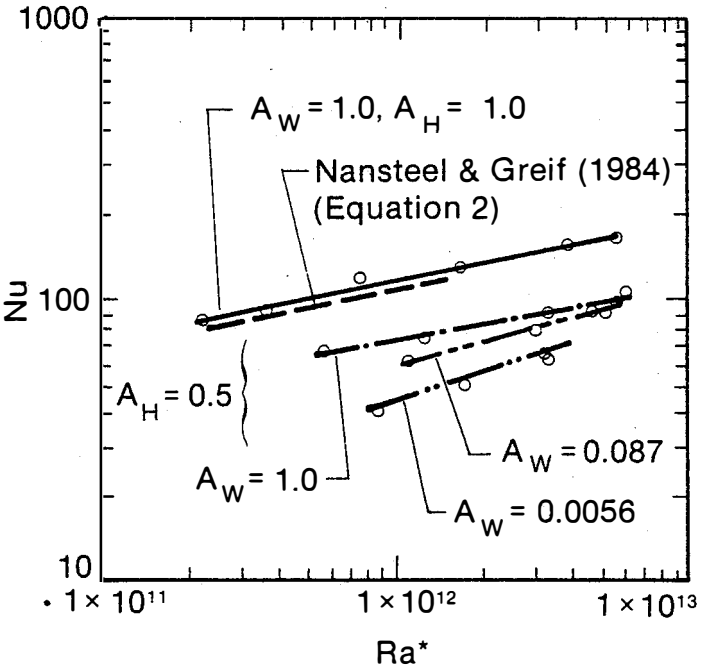


**Figure 5. Nusselt Number Correlations**

for $A_H$ = 0.5 and variable values of $A_W$. There is a dramatic drop in the Nusselt number when $A_H$ is decreased from 1 to 0.5 because of the relatively static pocket of hot fluid that is trapped in the upper half of the hot zone of the test cell. This trapped hot fluid inhibits heat transfer from the upper half of the hot wall.

Figure 5 demonstrates that when $A_W$ is reduced, the heat transfer between the hot and cold end walls is also reduced. Least squares fits to the experimental data in Fig. 5 produce the following correlations:

$$Nu = 0.324\ Ra^{*\,0.213},\ A_H = 1,\ A_W = 1 \quad (9)$$

$$Nu = 0.204\ Ra^{*\,0.213},\ A_H = 0.5,\ A_W = 1 \quad (10)$$

$$Nu = 0.030\ Ra^{*\,0.274},\ A_H = 0.5,\ A_W = 0.087 \quad (11)$$

$$Nu = 0.003\ Ra^{*\,0.351},\ A_H = 0.5,\ A_W = 0.0056 \quad (12)$$

As the aperture width ratio $A_W$ is decreased, there is an increase in the slope of the Nu vs. Ra* correlation, in addition to an overall reduction in heat transfer. This trend is consistent with the behavior predicted by Eq. (1) and Eq. (2). Selected results from Nansteel and Greif[17] are plotted in Fig. 5 for the case $A_H = 1$ (Eq 2).

## CONCLUSIONS

Experimental measurements have been conducted to determine the onset of blockage of a natural convection boundary layer flow through variable size aperture in a simple two-zone enclosure. The height of the aperture between zones was held constant at half the overall height of the enclosure while the width ratio of the aperture was varied over the range $1 \geq A_W \geq 0.0056$. The natural convection flow was driven by heating and cooling the end walls of the enclosure. Blockage of the boundary layer flow through the aperture was found to occur when the area of the aperture was reduced below a critical area which was approximately 2% of the total cross-sectional area of the test cell.

Blockage of the boundary layer flow caused a reduction in the level of thermal stratification in the hot zone, increased the temperature difference between the hot and cold zones, and reduced the convective heat transfer between the hot and cold end walls. The increase in the temperature difference between the hot and cold zones caused the aperture flow to change from a regime driven primarily by the boundary layers on the hot and cold walls to a regime driven primarily by the density differences between the two zones.

A simple model that predicts the onset of blockage of the boundary layer flow has been developed and shown to describe the major features of the blockage phenonemon. This study demonstrates that boundary layers can be used to transport energy without large bulk fluid temperature differences, provided that the flow aperture area is larger than the critical value for the onset of flow blockage. This result has important implications for the design of flow apertures in solar buildings and other applications that rely upon natural convection to transport energy between zones in multizone enclosures.

## ACKNOWLEDGMENT

This work was sponsored by the DOE Solar Buildings Program under contract DF-AC02-83CH10093. The first author gratefully acknowledges support provided by the SERI Summer Research Participant Program, which allowed him to conduct the research described in this paper at SERI during the summer of 1985.

## REFERENCES

1. Catton, I., "Natural Convection in Enclosures," 6th International Heat Transfer Conference, National Research Council of Canada, Toronto, 1978.

2. Ostrach, S., "Natural Convection Heat Transfer in Cavities and Cells," 7th Int. Heat Transfer Conference, Munich, Germany, 1982.

3. Churchill, S. W., "Free Convection in Layers and Enclosures," in Heat Exchanger Design Handbook, edited by E. U. Schlunder, Hemisphere Publishing, Washington, D. C., 1983.

4. Quintier, J., "Growth of Fire in Building Compartments," Fire Standards and Safety, ASTM STP 614, A. F. Robertson, Ed., American Society for Testing and Materials, 1977, pp. 131-167.

5. Yang, K. T., Lloyd, J. R., "Turbulent Flow in Vented Simple and Complex Enclosures," Natural Convection: Fundamentals and Applications, edited by S. Kakac, W. Aung, R. Viskanta, Hemisphere, 1985, pp. 303-329.

6. Thomas, P. H., Heselden, J. M., Law, M., "Fully-Developed Compartment Fires: Two Kinds of Behaviors," Fire Research Technical Paper No. 18, Fire Research Station, Borehamwood, England, October 1967.

7. Satoh, K., Lloyd, J. R. and Yang, K. T., "Turbulent Buoyant Flow and Smoke Layers in a Two-Dimensional Rectangular Compartment with Vertical Vents," Proceedings 1980 Fall Meeting of the Eastern Section of the Combustion Institute, Paper #22, 1980.
See also: Satoh, K., "Experimental and Finite Difference Study of Dynamic Fire Behaviors in a Cubic Enclosure with a Doorway," Report of Fire Research Institute of Japan, No. 55, 1983, pp. 17-29.

8. Brown, W. G., Solvason, K. R., "Natural Convection through Rectangular Openings in Partitions--1," Int. J. Heat Mass Transfer, Vol. 5, 1962, pp. 859-868.

9. Balcomb, J. D., Jones, G. F., Yamaguchi, K., "Natural Convection Airflow Measurement and Theory," Ninth National Passive Solar Conference, Columbus, Ohio, September 24-26, 1984.
See also: Jones, G. F., Balcomb, J. D and Otis, D. R. "A Model for Thermally Driven Heat and Air Transport in Passive Solar Buildings," ASME 85-WA/HT-69, 1985.

10. Kirkpatrick, A., Hill, D., Burns, P., "Interzonal Natural and Forced Convection Heat Transfer in a Passive Solar Building," to appear in ASME J. Solar Energy Engineering, 1986.

11. Jankowski, H. E., Ward, J., Probert, S. D., "Free Convection in Vertical Air-Filled Rectangular Cavities Filled with Baffles," 6th International Heat Transfer Conference, Toronto, 1978.

12. Bejan, A., Rossie, A. N., "Natural Convection in Horizontal Duct Connecting Two Fluid Reservoirs," J. Heat Transfer, Vol. 103, 1981, pp. 108-113.

13. Nansteel, M. W., Greif, R., "Natural Convection in Undivided and Partially Divided Rectangular Enclosures," J. Heat Transfer, Vol. 103, 1981, pp. 623-629.

14. Bajorek, S. M., Lloyd, J. R., "Experimental Investigation of Natural Convection in Partitioned Enclosures," J. Heat Transfer, Vol. 104, 1982, pp. 527-532.

15. Chang, L. C., Lloyd, J. R., Yang, K. T., "A Finite Difference Study of Natural Convection in Complex Enclosures," 7th International Heat Transfer Conference, Munich, Germany, 1982.

16. Lin, N. N., Bejan, A., "Natural Convection in a Partially Divided Enclosure," Int. J. Heat Mass Transfer, Vol. 26, 1983, pp. 1867-1878.

17. Nansteel, M. W., Greif, R., "An Investigation of Natural Convection in Enclosures with Two- and Three-Dimensional Partitions," Int. J. Heat Mass Transfer, Vol. 27, 1984, pp. 561-571.